JOURNAL OF APPLIED POLYMER SCIENCE VOL. 19, PP. 557-565 (1975)

Studies on Melt Spinning. V. Draw Resonance as a Limit Cycle

HIDEAKI ISHIHARA, *Katada Research Institute, Toyobo Co. Ltd., Ohtsushi 520-02, Japan* and SUSUMU KASE, *Technical Division, Toyobo Co., Osaka 530, Japan*

Synopsis

The exact wave form of draw resonance in isothermal spinning of Newtonian liquids was sought by solving numerically the simultaneous partial differential equations[1] of melt spinning in their original nonlinear form without recourse to perturbation. When the draw-down ratio of spinning exceeded 20, solution of the equations became a limit cycle, a sustained oscillation having amplitude and period independent of initial conditions. As the draw down ratio was further increased, the amplitude of the limit cycle grew very rapidly, and the wave form became close to a pulse train predicting an extreme thinning of the thread at regular intervals along the thread. The above solution for Newtonian liquids agreed well with experiment with respect to oscillation period. Agreement, however, was poor in amplitude, indicating that possibly the amplitude of draw resonance is affected by deviations of polymer viscosity from Newtonian.

INTRODUCTION

In a previous study,[1] one of the authors discussed the stability of melt spinning using linearized perturbation equations derived from the partial differential equations of melt spinning introduced in the first of this study series.[2] For brevity, we call hereafter the latter of the above equations simply equations of melt spinning.

The perturbation equations are quite useful in discussing the conditions of spinning instability or in approximately predicting the oscillation period, but they fail to simulate the amplitude and wave form of draw resonance encountered in physical systems since the perturbation equations are linearized approximations meant just for small deviations from the steady state values. Being linear, the perturbation equations, when unstable, give a solution growing without bound, whereas the physical draw resonance is a standing oscillation of fixed amplitude and period often encountered in nonlinear systems. When a nonlinear differential equation has a solution in the form of a standing oscillation having amplitude and period independent of initial conditions, the solution is called a limit cycle.[3] The equations of melt spinning are nonlinear and are supposedly capable of simulating the phenomenon of draw resonance. Therefore, their solution for an unstable spinning condition should become a limit cycle.

In the present study, on account of this, we solve numerically the equations of melt spinning in their original nonlinear form to seek to obtain the exact theoretical wave form of draw resonance in the isothermal spinning of Newtonian liquids. Solutions are then compared with experiments.

Although discussions are limited to isothermal spinning, results can at least qualitatively be applied to the nonisothermal case, since we found[1] that draw resonance can occur only when the spinning is carried out under approximately isothermal conditions.

NUMERICAL COMPUTATION OF LIMIT CYCLE SOLUTIONS

Equations of melt spinning under isothermal conditions take the form

$$\frac{\partial v}{\partial x} = \frac{F}{A\beta} \tag{1}$$

$$\frac{\partial A}{\partial \tau} + \frac{\partial}{\partial x}(Av) = 0 \tag{2}$$

where τ is time, x is distance from spinneret, A is cross-sectional area, v is velocity in the x direction, F is thread tension, and β is Trouton viscosity assumed constant under isothermal conditions (see Fig. 1).

Boundary conditions applicable are: (i) fixed velocity v_{00}, and cross-sectional area A_{00}, near the spinneret, where subscript 00 denotes the value at the position of maximum diameter; (ii) fixed take-up speed, v_w, where the subscript w denotes the value at the take-up point.

Equations (1) and (2) are first converted into nondimensional form by defining the following variables:

$$\zeta = x/x_w = \text{nondimensional distance} \tag{3}$$

$$\tau^* = \tau v_{00}/x_w = \text{nondimensional distance time} \tag{4}$$

$$\lambda = A/A_{00} = \text{nondimensional distance thread cross-sectional area} \tag{5}$$

$$\psi = v/v_{00} = \text{nondimensional distance thread velocity} \tag{6}$$

$$\xi = Fx_w/(A_{00}v_{00}\beta) = \text{nondimensional distance tension} \tag{7}$$

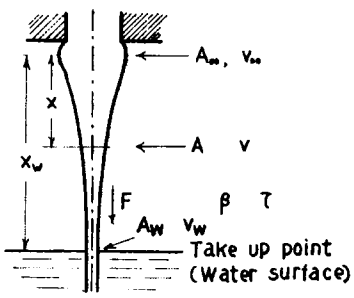

Fig. 1. Schematic diagram of water-quenched melt spinning.

Equations (1) and (2) now become

$$\lambda \frac{\partial \psi}{\partial \zeta} = \xi \tag{8}$$

$$\frac{\partial \lambda}{\partial \tau^*} + \psi \frac{\partial \lambda}{\partial \zeta} = -\xi. \tag{9}$$

Steady-state solutions of eqs. (8) and (9), denoted by subscript 0, are

$$\psi_0 = e^{b\zeta} \tag{10}$$

$$\lambda_0 = e^{-b\zeta} \tag{11}$$

where b is the natural logarithm of draw down ratio, ψ_w, and is the only parameter in this system. For an easy visualization of solutions, dependent variables ψ and λ in eqs. (8) and (9) are converted into ratios V and W over the respective steady-state values ψ_0 and λ_0:

$$\psi = V\psi_0 \tag{12}$$

$$\lambda = W\lambda_0 \tag{13}$$

The dimensionless distance ζ, too, is replaced with the dimensionless flow-down time ζ^* defined in eq. (14) below in order to simplify mathematical expression:

$$\zeta^* = \int_0^\zeta \frac{1}{\psi_0} d\zeta = \frac{1}{b}(1 - e^{-b\zeta}). \tag{14}$$

The dimensionless flow-down time ζ^* is equivalent to the time the polymer takes under steady-state condition to flow down from the position of maximum diameter to position ζ and made dimensionless by multiplying (v_{00}/x_w).

By substituting eqs. (12), (13), and (14) into eqs. (8) and (9), we get

$$\frac{\partial V}{\partial \zeta^*} + \frac{b}{1 - b\zeta^*} V = \frac{\xi}{W} \frac{1}{1 - b\zeta^*} \tag{15}$$

$$\frac{\partial W}{\partial \tau^*} + \frac{\partial}{\partial \zeta^*}(VW) = 0. \tag{16}$$

The value of ζ^* at the take-up point is

$$\zeta_w^* = \frac{1}{b}(1 - e^{-b}). \tag{17}$$

Equations (15) and (16) are then converted into difference equations using the backward difference scheme given below:

$$V \rightarrow V_{i+1,j+1} \tag{18}$$

$$W \rightarrow W_{i+1,j+1} \tag{19}$$

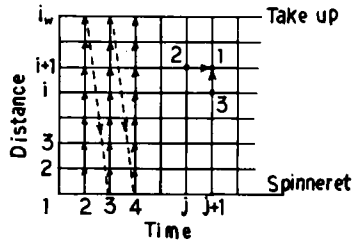

Fig. 2. Procedure of numerical computation.

$$\frac{\partial V}{\partial \zeta^*} \rightarrow (V_{i+1,j+1} - V_{i,j+1})/\Delta \tag{20}$$

$$\frac{\partial W}{\partial \tau^*} = (W_{i+1,j+1} - W_{i+1,i})/\Delta \tag{21}$$

$$\frac{\partial}{\partial \zeta^*}(VW) \rightarrow (V_{i+1,j+1}\, W_{i+1,j+1} - V_{i,j+1}\, W_{i,j+1})/\Delta \tag{22}$$

where i and j are increment numbers, respectively, in the ζ^* and the τ^* directions as shown in Figure 2. Equations (15) and (16) reduce to

$$V_{i+1,j+1} = (1 + F_1F_3)/(F_1F_2 - 1) \tag{23}$$

$$W_{i+1,j+1} = (F_1F_2 - 1)/(F_2 + F_3) \tag{24}$$

where

$$F_1 = W_{i+1,j} + V_{i,j+1}\, W_{i,j+1} \tag{25}$$

$$F_2 = (1 - b\zeta^*)/(\xi\Delta) + b/\xi \tag{26}$$

$$F_3 = (1 - b\zeta^*)\, V_{i,j+1}/(\xi\Delta). \tag{27}$$

Referring to Figure 2, eqs. (23) through (27) enable the computation of the values of V and W at point 1 when V and W are known at points 2 and 3. Computations, therefore, can proceed along the dotted lines in Figure 2. However, computations under each j value must be iterated by modifying the value of nondimensional tension ξ using Newton's method[4] until the boundary condition at the take-up point is satisfied.

A computer program having 71 FORTRAN statements has been developed to execute the above computations. It took approximately 5 min on an IBM 370/155 computer to carry out the computations for one spinning condition when the number of mesh points as shown in Figure 2 were 100 (i) $\times$ 7000 (j) = 7×10^5.

DISCUSSION ON LIMIT CYCLE SOLUTIONS

Computed solutions of eqs. (23) and (24) corresponding to five different b values, 2.0, 3.0, 3.5, 4.0, and 4.5, and expressed in terms of nondimensional cross-sectional area W_w at the take-up versus j are shown in Figures 3 (a)

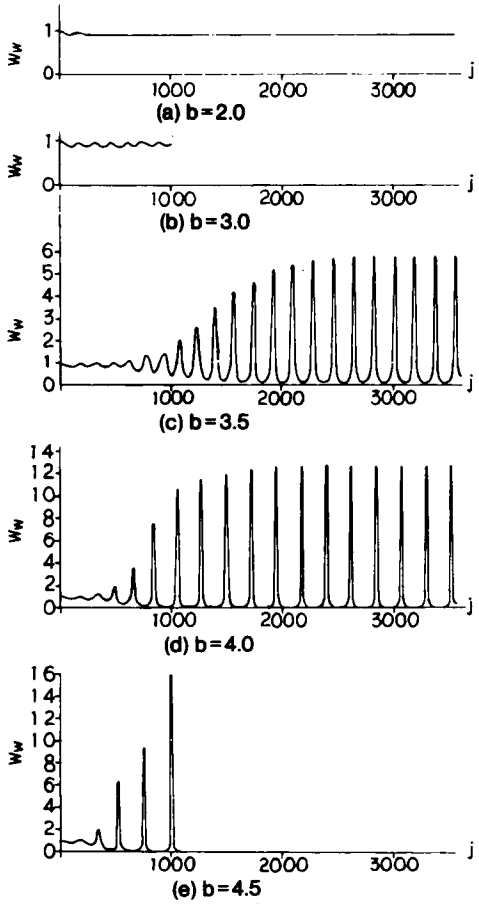

Fig. 3. Computed thread thickness at take-up point vs. time increments j.

through 3 (e). The value of Δ was $\zeta_w^*/100$. This makes $j = 100$ correspond to $\zeta^* = \zeta_w^*$, or the time the polymer takes to flow down from the spinneret to the take-up point under steady-state condition.

Initial and boundary conditions used were:

$$V = W = 1.0 = \text{steady-state values} \qquad \text{at } \tau^* = 0 \tag{28}$$

$$V = W = 1.0 = \text{steady-state values} \qquad \text{at } \zeta^* = 0 \tag{29}$$

$$V_w = 1.0 + 0.1\, u(\tau^*) \qquad \text{at } \zeta^* = \zeta_w^* \tag{30}$$

where $u(\ )$ is the unit step function.

Equations (28) through (30) signify that the system was at steady state initially and a step increase of 0.1 $u(\tau^*)$ in take-up speed is exerted as an external disturbance. Because of this 10% increase in take-up speed, the solutions shown in Figure 3, in fact, correspond to effective log draw-down ratios of 2.095, 3.095, 3.595, 4.095, and 4.595 rather than 2.0, 3.0, etc.

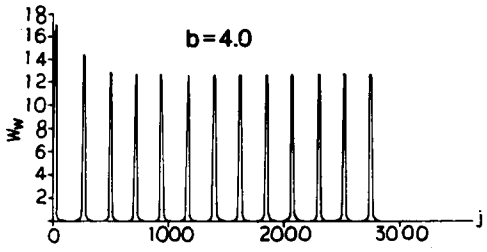

Fig. 4. Solution for $b = 4.0$ as in Fig. 3(d) but under different initial condition.

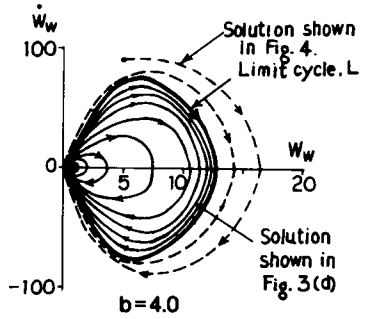

Fig. 5. Proof of the existence of limit cycle.

In what follows are discussions on the curves shown in Figure 3.

(i) When the log draw-down ratio, b, exceeds 3.0, the solution starts to settle to a sustained oscillation. This is in agreement with the previous[1] perturbation analysis which showed that isothermal spinning becomes unstable at $b = 3.0$.

(ii) The sustained oscillations shown in Figure 3(b) through 3(e) are limit cycles. The proof for this is as follows. Shown in Figure 4 is a solution W_w for $b = 4.0$ as in Figure 3(d) but starting from a different initial condition, $W = 1 + 4\zeta$ and $V_w = 1 + 0.1\, u(\tau^*)$. It is evident that the standing oscillation part of the curve in Figure 4 is identical in wave form to that in Figure 3(d). The standing oscillation is independent of initial condition, hence is a limit cycle. The existance of limit cycle can more clearly be visualized by plotting the above two solutions on a W_w-versus-$\dot{W}_w$ diagram as shown in Figure 5. $\dot{W}_w$ is the time derivative of W_w. The solution shown in Figure 3(d) starts at a point inside the closed path L in Figure 5, takes a divergent path, and eventually settles to L, whereas the solution shown in Figure 4 converges to L from outside. This establishes the existence of limit cycle L.

(iii) As the value of b increases beyond 3.0, the amplitude of the limit cycle increases sharply and the minimum thread thickness quickly approaches zero, as shown graphically in Figure 6.

(iv) When b is more than about 3.5, the limit cycle practically takes the form of a pulse train with most of the thread mass concentrated at the peaks.

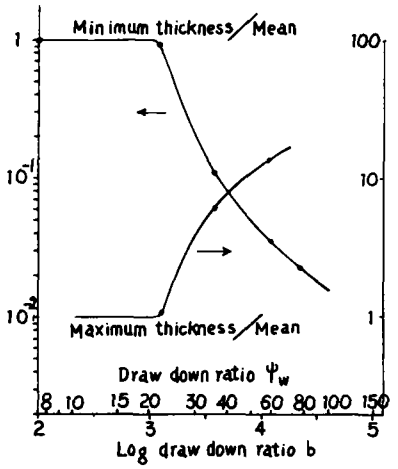

Fig. 6. Maximum and minimum thread thickness vs. log draw-down ratio b.

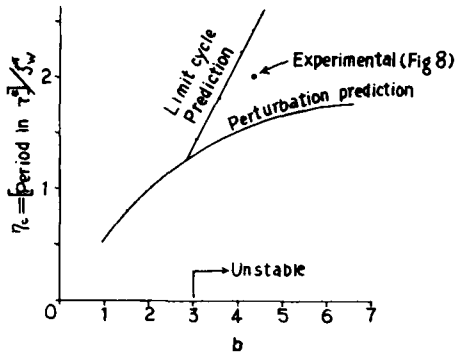

Fig. 7. Nondimentional oscillation period η_c vs. b.

(v) In a previous paper,[1] the period of linearized oscillation was expressed as a multiple η_c of dimensionless flow-down time, ζ_w^*, and was given as a function of log draw-down ratio b as reproduced in Figure 7. The period η_c^* of limit cycle coincides with η_c at the critical b value of $b = 3.0$ where the limit cycle starts to appear. However, as shown in Figure 7, η_c^* quickly deviates from η_c as the amplitude of the limit cycle grows with increasing b.

COMPARISON WITH EXPERIMENTS

The draw resonance in water-quenched melt spinning of PET discussed in a previous paper[1] is reproduced in Figure 8. Spinning conditions relevant to the present study are:

$$\text{air gap, } x_w = 2.0 \text{ cm}$$

$$\text{log draw-down ratio, } b = 4.33$$

$$\text{take-up velocity, } v_w = 500 \text{ cm/sec.} \tag{31}$$

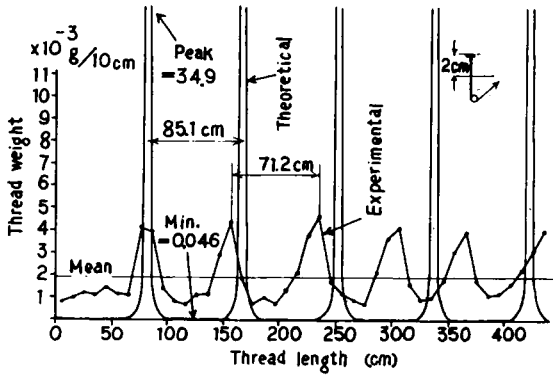

Fig. 8. Draw resonance in water-quenched melt spinning of PET compared with corresponding theoretical curve for Newtonian liquids.

The corresponding limit cycle solution was superposed on the experimental curve in Figure 8. The mean value of the theoretical curve in Figure 8 is made to coincide with that of the experimental curve. The dimensionless time τ^* for the theoretical curve was converted into thread length L using eq. (4) and the relation

$$L = v_w \tau. \tag{32}$$

The theoretical oscillation period agrees fairly well with the experimental value. In fact, the experimental value falls between the linearized prediction and the limit cycle prediction, as shown in Figure 7. This might be expected, since the two predictions correspond respectively to very small and very large amplitudes and the experimental draw resonance has a medium amplitude.

As far as the amplitude is concerned, however, there is a large discrepancy between limit cycle theory and experiment. This discrepancy most likely reflects the deviation of polymer rheology from that of Newtonian liquids. Since the limit cycle shown in Figure 8 is the "exact" solution of eqs. (1) and (2) for $b = 4.33$, it should show how Newtonian liquids behave under this spinning condition. Therefore, it is desirable to introduce rheological equations such as the power law model or the Maxwell model into the right-hand side of eq. (1) so that experiments can better be simulated. It also leads to the idea that the tensile rheology of polymers might be measured indirectly by observing the shape of draw resonance.

Shown in Figure 9 is draw resonance under three different draw-down ratios observed in the water-quenched melt spinning of PP monofilament using the experimental setup shown in Figure 10. Since these experiments were not carried out under fully isothermal conditions, the curves cannot be compared with the theoretical values directly. Figure 9, however, clearly exhibits the theoretically predicted tendency that the wave form of draw resonance approaches a pulse train with increasing b.

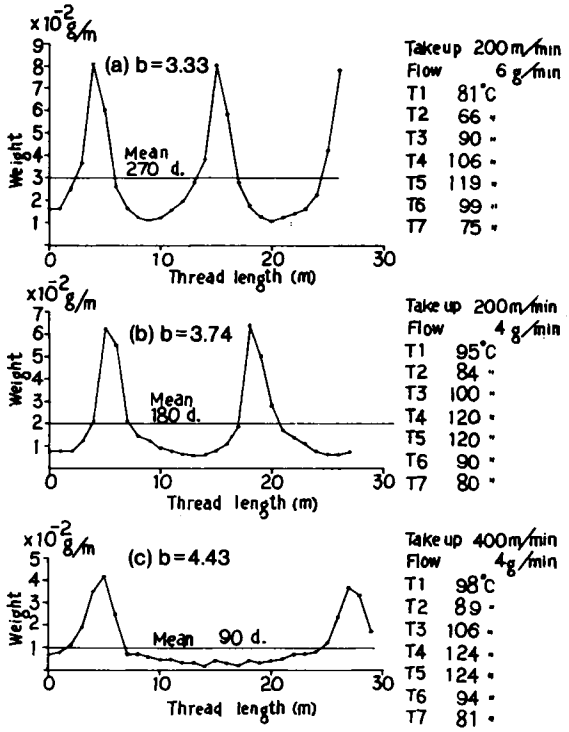

Fig. 9. Wave form of draw resonance in water-quenched melt spinning of PP approaches pulse train with increasing b. See Fig. 10 for spinning setup.

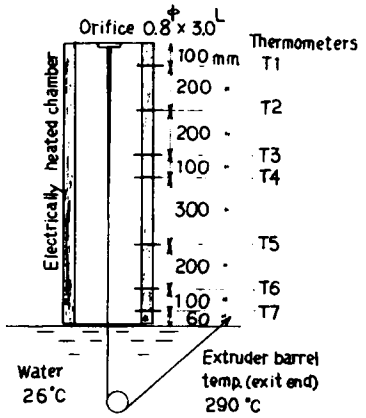

Fig. 10. Water-quenched melt spinning of PP.

CONCLUSIONS

Equations of melt spinning in their original nonlinear form were found to yield limit cycle solutions clarifying the standing oscillation feature of the phenomenon of draw resonance. The amplitude of the limit cycle solution for isothermal Newtonian liquids, however, was much larger than the cor-

responding experimental value for PET yarn, suggesting that the amplitude of draw resonance may be quite sensitive to the tensile rheology of polymers.

The authors are grateful to Mr. H. Yasuda, Mr. K. Tani, and Mr. T. Ueyama, all of Toyobo Co. Ltd., for their cooperation in experiments and machine computations.

References

1. S. Kase, *J. Appl. Polym. Sci.*, **18**, 3279 (1974).
2. S. Kase and T. Matsuo, *J. Polym. Sci. A*, **3**, 2541 (1965).
3. J. G. Truxal, *Automatic Feedback Control System Synthesis*, McGraw-Hill, New York, 1955, pp. 641–645.
4. R. G. Stanton, *Numerical Methods for Science and Engineering*, Prentice-Hall, Princeton, New Jersey, 1961, pp. 84–89.

Received June 13, 1974
Revised August 14, 1974